Research Networking Programmes

Short Visit Grant ☐ or Exchange Visit Grant ☒

(please tick the relevant box)

Scientific Report

Scientific report (one single document in WORD or PDF file) should be submitted online within one month of the event. It should not exceed eight A4 pages.

***Proposal Title*: "Electromagnetic properties of a thin dielectric disk sandwiched between two graphene covers with applications to tuneable THz filters"**

***Application Reference N°*: 4147**

1) Purpose of the visit

The main idea of the proposed research was to study numerically tunability of the resonance frequencies of a thin dielectric disk covered with two graphene layers. Graphene, which is a planar hexagonal structured layer of carbon atoms, is a very promising material in nanoelectronics. It is a zero bandgap semiconductor with conductivity tuned either by electrostatic or magnetostatic gating. Graphene layer located in free space or in a dielectric host medium supports surface-plasmon waves in the terahertz range, the properties of which depend on the properties of the host medium and graphene conductivity. In the project work, we proposed to investigate the emission and absorption of waves generated by a point source in the presence of a single graphene disk and a thin dielectric disk covered with graphene on two flat sides. Such structures are of interest for several reasons. First of all this needs a graphen layer and its conductivity model to be incorporated into electromagnetic boundary-value problem. Secondly the excitation of plasmon resonances on graphen disks allows designing a tuneable open resonator in the terahertz frequency range. This tunability can be provided in more realistic way and even be greatly enhanced if two graphene screens sandwich a thin dielectric disk.

The study is based on the full-wave analysis using the method of analytical regularization (MAR) developed earlier for a thin dielectric disk. In part, this development was performed during my previous NEWFOCUS exchange-visit travel grant to Universite de Rennes 1 in 2011.

Later I have developed an analytical-numerical method for the study of electromagnetic wave scattering by a thin graphene disk. We suppose that the radius of graphene disk is larger than 50 nm and thus disregard the edge effects on the graphene conductivity and use the electrical conductivity model developed for infinite graphene sheets. To solve Maxwell boundary value problem we have to derive a set of dual IEs in the spectral domain. That enables us to reduce the problem to another set of the Fredholm second kind IEs on the semi-infinite interval for the unknown images of the normal to the disk field components. The features of such equations guarantee the existence and

uniqueness of their exact solution, thus one can use simple schemes to solve them numerically. We use a convergent and economic Nystrom-type discretization to obtain the final matrix equation.

2) Description of the work carried out during the visit and the main results obtained

Mathematical Models of Graphene Layer and Sandwich Layer

To study electromagnetic wave scattering by graphene objects is necessary to couple the Maxwell's boundary value problem with phenomenological model of graphene conductivity. The main challenge of such approach is to involve zero thickness of the scatter into the model. This can be done by approximating the graphene slab with an equivalent thin layer with finite thickness. However such approach leads to the computational disaster due to very high length-to-thickness ratio (and thus very large size of matrix to be inverted). A way out of this is to model graphene as an equivalent zero-thickness resistive (also called impedance) surface.

Consider the scattering of the time-harmonic ($e^{-i\omega t}$) electromagnetic field of an elementary dipole by a graphene or graphene-dielectric-graphene (GDG) sandwiched disk with radius a (Fig. 1). Suppose the dipole is located at the distance h above the disk and is shifted from the disk axis at the distance r_0. In our analysis, we will use the dimensionless, i.e. normalized to the radius of the disk cylindrical coordinates (ρ,φ,ζ) with the origin in the centre of the disk. Decompose the total field as a sum of the incident and the scattered by the disk electromagnetic fields. Assume that that the scattered field satisfies homogeneous Maxwell equations outside the disk, while the total field satisfies the following two-side generalized boundary conditions:

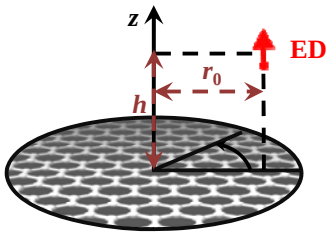

Figure 1. Micro-size graphene disk

a) on a single graphene disk,

$$\left(E_{tg}^{+}+E_{rg}^{-}\right)=2\sigma_{Gr}^{-1}\vec{n}\times\left(H_{tg}^{+}-H_{tg}^{-}\right),\qquad \left(E_{tg}^{+}-E_{rg}^{-}\right)=0 \tag{1}$$

b) on the median plane of a graphene-sandwiched dielectric disk,

$$\left(E_{tg}^{+}+E_{tg}^{-}\right)=2R_{eff}Z_0\vec{n}\times\left(H_{tg}^{+}-H_{tg}^{-}\right) \tag{2}$$

$$Z_0\left(H_{tg}^{+}+H_{tg}^{-}\right)=-2Q_{eff}\vec{n}\times\left(E_{tg}^{+}-E_{tg}^{-}\right) \tag{3}$$

In (1), Z_0 is the free-space impedance, $\vec{n}$ is the normal to the disk surface unit vector, and σ is the graphene surface conductivity. This quantity can be determined from the Kubo formalism and expressed as a sum of intraband (σ_{intra}) and interband (σ_{inter}) contributions given by the following expressions:

$$\sigma_{\text{intra}}=\frac{i\,e^2k_BT}{\pi\hbar(\omega+i/\tau)}\left\{\frac{\mu_c}{k_BT}+2\ln\left[\exp\left(-\frac{\mu_c}{k_BT}\right)+1\right]\right\}, \tag{4}$$

$$\sigma_{\text{inter}}=\frac{i\,e^2(\omega+i/\tau)}{\pi\hbar^2}\int_0^{\infty}\frac{f_d(-\varepsilon)-f_d(\varepsilon)}{(\omega+i/\tau)^2-4(\varepsilon/\hbar)^2}\,d\varepsilon\,, \tag{5}$$

where e is the charge of an electron, k_B is the Boltzmann constant, T is temperature, $\hbar$ is the reduced Planck constant, ω is the angular velocity, τ is the relaxation time of an electron, μ_c is the chemical potential and f_d is the Fermi-Dirac distribution function. Besides, here R_{eff} and Q_{eff} are effective electrical and magnetic resistivities, which depend on the permittivity of dielectric material, graphene conductivity, frequency of the incident field, and sandwiched disk thickness. Expressions for effective

resistivities will be obtained below. Note that the resistive-type two-side boundary conditions (1) are a limiting case of the generalized boundary conditions (2), (3) for $R_{eff} \doteq R_{Gr} = 1/(Z_0 \sigma_{Gr})$, $Q_{eff} = 0$.

To find effective resistivities for a GDG disk, we follow the following procedure:

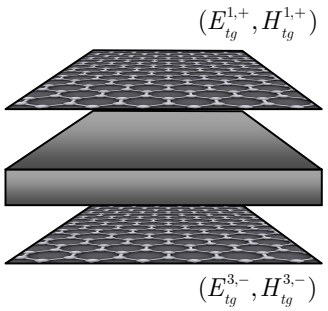

Figure 2. Split layers

- At first, we split the whole sandwich into three single layers (Fig. 2) and suppose there are non-zero free space gaps between each of layers. Define $(E_{tg}^{1,+}, H_{tg}^{1,+})$ and $(E_{tg}^{1,-}, H_{tg}^{1,-})$ as the limits of the tangential to the layer field components at the top and the bottom sides of the top layer, respectively. Also define $(E_{tg}^{2,+}, H_{tg}^{2,+})$ and $(E_{tg}^{2,-}, H_{tg}^{2,-})$ as the limits of the tangential field components at the top and the bottom surfaces of dielectric layer. Finally, define $(E_{tg}^{3,+}, H_{tg}^{3,+})$ and $(E_{tg}^{3,-}, H_{tg}^{3,-})$ as the limit values of the field components at the bottom-graphene-layer top and bottom sides, respectively.
- Consider the following boundary conditions:

$$\left(E_{tg}^{1,+} + E_{tg}^{1,-}\right) = 2\sigma_{Gr}^{-1} \cdot \vec{n} \times \left(H_{tg}^{1,+} - H_{tg}^{1,-}\right), \qquad \left(E_{tg}^{1,+} - E_{tg}^{1,-}\right) = \vec{0}, \tag{6}$$

$$\begin{aligned} \left(E_{tg}^{2,+} + E_{tg}^{2,-}\right) &= 2Z_0 R_{Diel} \cdot \vec{n} \times \left(H_{tg}^{2,+} - H_{tg}^{2,-}\right), \\ \left(E_{tg}^{2,+} - E_{tg}^{2,-}\right) &= Z_0/2\, Q_{Diel}^{-1} \cdot \vec{n} \times \left(H_{tg}^{2,+} + H_{tg}^{2,-}\right), \end{aligned} \tag{7}$$

$$\left(E_{tg}^{3,+} + E_{tg}^{3,-}\right) = 2\sigma_{Gr}^{-1} \cdot \vec{n} \times \left(H_{tg}^{3,+} - H_{tg}^{3,-}\right), \qquad \left(E_{tg}^{3,+} - E_{tg}^{3,-}\right) = \vec{0}. \tag{8}$$

They are conditions for the electromagnetic field on a graphene layer (6), (8) and two-side GBC for a thin dielectric layer (7). Here, R and Q are the electric and magnetic resistivities given as $R = iZ/2\cot(\sqrt{\varepsilon_r \mu_r}\, k\tau/2)$, $Q = R/Z^2$ if $k\tau \ll 1$ and $\left|\varepsilon_r \mu_r\right| \gg 1$, Z_0 is the free-space impedance, Z is the relative impedance of the disk material, $k = \omega/c$ is the wavenumber, ε_r and μ_r are the relative permittivity and permeability, respectively.

- Assume that the thicknesses of each gap tend to zero. Then $(E_{tg}^{1,-}, H_{tg}^{1,-}) = (E_{tg}^{2,+}, H_{tg}^{2,+})$ and $(E_{tg}^{2,-}, H_{tg}^{2,-}) = (E_{tg}^{3,+}, H_{tg}^{3,+})$ and after some algebraic transformations we obtain the following:

$$\left(E_{tg}^{1,+} + E_{tg}^{3,-}\right) = 2Z_0 R_{GDG} \cdot \vec{n} \times \left(H_{tg}^{1,+} - H_{tg}^{3,-}\right), \tag{9}$$

$$\left(E_{tg}^{1,+} - E_{tg}^{3,-}\right) = Z_0/2\, Q_{GDG}^{-1} \cdot \vec{n} \times \left(H_{tg}^{1,+} + H_{tg}^{3,-}\right), \tag{10}$$

where

$$R_{GDG} = R_{Diel} / \left(2R_{diel} / R_{Gr} + 1\right), \; Q_{GDG} = 1/2R_{Gr} + Q_{Diel} \tag{11}$$

Thus we have obtained the two-side GBCs for the tangential to the layer field components. They can be used for the modelling of a graphene-dielectric-graphene sandwich layer. The use of these two-side GBCs enables one to exclude from consideration the field inside the sandwich while solving the scattering problem.

- By the similar but reverse procedure one can modify the obtained two-side GBCs so that the sandwiched layer can be reduced to a boundary of zero thickness. Finally, that leads to the effective GBC (2) and (3) at the median section of the layer with effective resistivities given by the following expressions:

$$R_{eff}=\frac{4Q_0R_0R_{GrDielGr}+R_{GrDielGr}-2R_0}{4Q_0R_0-8Q_0R_{GrDielGr}+1},\quad Q_{eff}=\frac{4R_0Q_0Q_{GrDielGr}+Q_{GrDielGr}-2Q_0}{4R_0Q_0-8R_0Q_{GrDielGr}+1}, \tag{12}$$

where $R_0=Q_0=i\cot\left(k\tau/4\right)/2$ and $R_{GrDielGr}$, $Q_{GrDielGr}$ are given by (11).

Integral equations and numerical solution method

For uniqueness, we additionally request the total field to satisfy the radiation condition and the condition of local integrability of power. We also assume that the scattered field is continuous everywhere outside the disk. To apply the MAR developed earlier for a dielectric disk scattering problem, it is necessary to supplement GBC (1)-(3) with the condition of the absence of equivalent currents out of disk's surface in the plane of its median section $(\zeta=0,\rho>1)$.

To solve the 3-D scattering problem by a disk, we use the method of the dual integral equations (IEs) in the spectral domain together with the concept of analytical regularization. The following expressions for the normal and tangential to the disk scattered-field components in terms of the scalar and vector Fourier-Hankel transform are used to satisfy analytically the Maxwell equations and the condition of radiation at infinity:

$$\begin{pmatrix}E_z^{sc,\pm}(\rho,\varphi,\zeta)\\ Z_0H_z^{sc,\pm}(\rho,\varphi,\zeta)\end{pmatrix}=\sum_{m=-\infty}^{\infty}e^{im\varphi}\int_0^{\infty}e^{i\gamma(\kappa)|\zeta|}J_{|m|}(\kappa\rho)\begin{pmatrix}\kappa e_{m,z}^{sc,\pm}(\kappa)\\ \kappa h_{m,z}^{sc,\pm}(\kappa)\end{pmatrix}d\kappa, \tag{13}$$

$$\begin{pmatrix}E_r^{sc,\pm}(\rho,\varphi,\zeta)\\ -iE_\varphi^{sc,\pm}(\rho,\varphi,\zeta)\end{pmatrix}=\sum_{m=-\infty}^{\infty}e^{im\varphi}\int_0^{\infty}e^{i\gamma(\kappa)|\zeta|}\bar{H}_m(\kappa\rho)\begin{pmatrix}\pm i\gamma(\kappa)e_{m,z}^{sc,\pm}(\kappa)\\ -ka\,h_{m,z}^{sc,\pm}(\kappa)\end{pmatrix}d\kappa \tag{14}$$

$$\begin{pmatrix}Z_0H_r^{sc,\pm}(\rho,\varphi,\zeta)\\ -iZ_0H_\varphi^{sc,\pm}(\rho,\varphi,\zeta)\end{pmatrix}=\sum_{m=-\infty}^{\infty}e^{im\varphi}\int_0^{\infty}e^{i\gamma(\kappa)|\zeta|}\bar{H}_m(\kappa\rho)\begin{pmatrix}\pm i\gamma(\kappa)h_{m,z}^{sc,\pm}(\kappa)\\ ka\,e_{m,z}^{sc,\pm}(\kappa)\end{pmatrix}d\kappa \tag{15}$$

Here, $\gamma(\kappa)=[(ka)^2-\kappa^2]^{1/2}$ is the complex-valued function with the branch corresponding to $\mathrm{Im}(\gamma(\kappa))\geq 0$, k is the free-space wavenumber, and $\bar{H}_m(\kappa\rho)$ is the matrix kernel of the vector Hankel transform given by

$$\bar{H}_m(\kappa\rho)=\begin{pmatrix}J'_{|m|}(\kappa\rho) & mJ_{|m|}(\kappa\rho)/(\kappa\rho)\\ mJ_{|m|}(\kappa\rho)/(\kappa\rho) & J'_{|m|}(\kappa\rho)\end{pmatrix}, \tag{16}$$

where $J_m(\cdot)$ is the Bessel function of the order *m*, $J'_m(\cdot)$ its first-order derivative, and $e_{m,z}^{sc,\pm}(\kappa)$ and $h_{m,z}^{sc,\pm}(\kappa)$ are the spectral-domain images of the field components normal to the disk.

By substitution of the expressions (14), (15) into the GBC we reduce the problem to a set of dual IEs (for each azimuthal index *m*) for the unknowns, which are the images of the jumps and the average values of the scattered field components normal to the disk. Then, following the MAR developed earlier for a thin dielectric disk and inverting the most singular part of IEs, we reduce the scattering problem to a set of the Fredholm second kind IEs on the semi-infinite interval. The features of such equations guarantee the existence and uniqueness of their exact solution. To solve them we use a numerical technique which is based on the truncation of the integration interval to the finite one combined with the discretization of the truncated equations by a Nystrom-type scheme. Finally we obtain a set of linear algebraic equations and solve it numerically using the Gauss inversion of the corresponding matrix.

Numerical results

a) Single graphene disk

To study the excitation of the graphene-disk plasmon resonances by the point sources (see Fig. 1), we chose, as the figures-of-merit, the power radiated by the chosen source in the presence of the graphene disk and the power lost due to absorption. The both values will be normalized by the power

radiated by the same source located in free space. We have considered two types of dipoles, namely a horizontal magnetic dipole and a vertical electric dipole. Our aim is to study the excitation of the graphene plasmon resonances as the source of the incident field shifts from the disk axis toward the rim of the disk. Besides, we analyze how the resonances shift if the chemical potential gets larger.

We start our consideration with the dipoles located on the disk axis ($r_0 = 0$) and change the chemical potential of the graphene μ_c from 0.25 to 1.0 eV. Fig. 3 shows the normalized radiated and absorbed powers as a function of the frequency in the case of a horizontal magnetic dipole excitation.

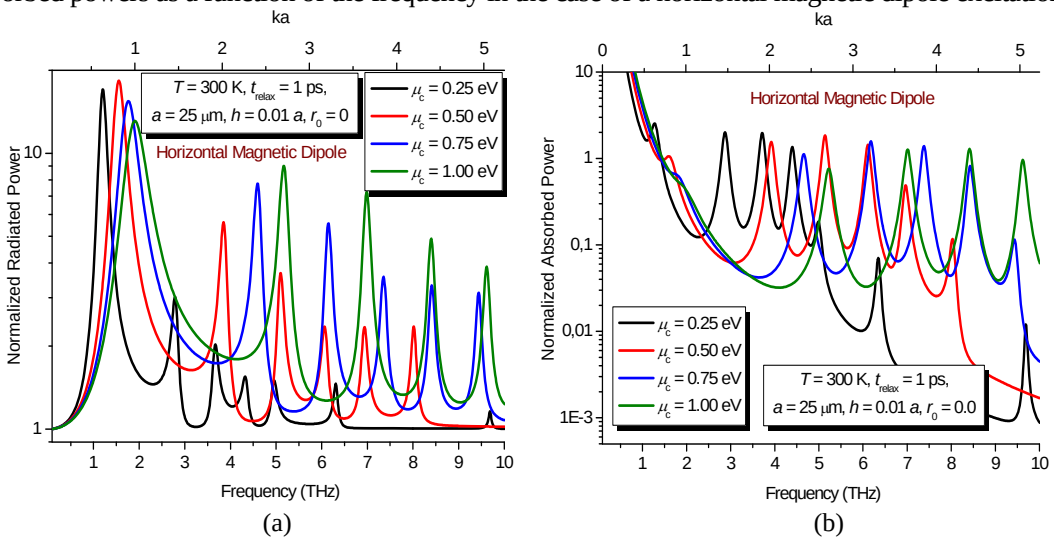

Figure 3. Normalized radiated and absorbed powers versus the frequency for the graphene disk (a = 25 μm) excited by the on-axis horizontal magnetic dipole.

One can see several resonance peaks on each curve. They correspond to the family of standing-wave plasmon resonance modes with one variation of the field along the disk azimuth and several variations along the disk radius. Thus, for example, the resonance frequency f = 1.5425 THz for the red curve in Fig. 3(a) corresponds to the resonance mode with a single variation of the field along the azimuth (without variation along the radius). A typical far field pattern in such resonance looks like the pattern in Fig. 5(d). Also note the up-shifting of the resonance frequencies when the graphene chemical potential gets larger (this is the same as increasing the electrical bias of the graphene material).

Fig. 4(a) shows frequency dependences of the normalized radiated power for the same parameters of graphene disk but in the case of the on-axis vertical electrical dipole excitation. Such incident field has no variations along the azimuth and thus it excites only azimuthally-symmetric (m = 0) surface plasmon modes. Figs. 5(a)-5(c) show the radiation patterns at three resonance frequencies, f = 3.1368 THz, 4.5512 THz and 9.3182 THz for the red curve (which corresponds to the graphene chemical potential of 0.5 eV) in Fig. 4(a).

Fig. 4(b) shows frequency dependences of the normalized radiated power for several different source-point locations. Here, we start shifting the vertical electrical dipole from the axis of the disk to the rim and observe excitation of cylindrical standing-wave plasmon modes of different azimuthal families ($m = 0;1;2;\ldots$).

According with the conception of effective refractive index of a thin-disk resonator, the plasmon-resonance frequencies of a stand-alone graphene disk can be found from the approximate characteristic equation as follows:

$$J_m\left(\alpha_p a\right) \approx 0, \quad m = 0;1;2;\ldots\ , \tag{17}$$

where $\alpha_P = k\sqrt{1-(\sigma Z_0/2)^2}$ is the propagation constant of a surface-plasmon wave supported by the infinite layer of graphen suspended in free space.

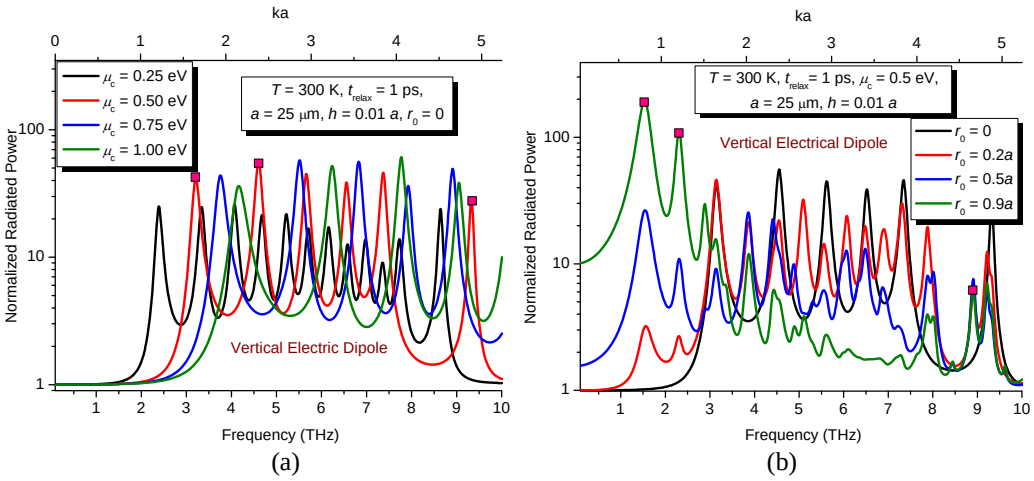

Figure 4. Normalized radiated powers versus the frequency for the graphene disk (a = 25 μm) excited by the on-axis (a) and the shifted (b) vertical electric dipoles.

The 3-D far-field radiation patterns presented in Figs. 5(d)-5(f) have been computed at three resonance frequencies f = 1.5425 THz, 2.3071 THz and 8.9016 THz corresponding to the excitation of the plasmon modes with $m = 1;2;4$ and marked in Fig. 4(b).

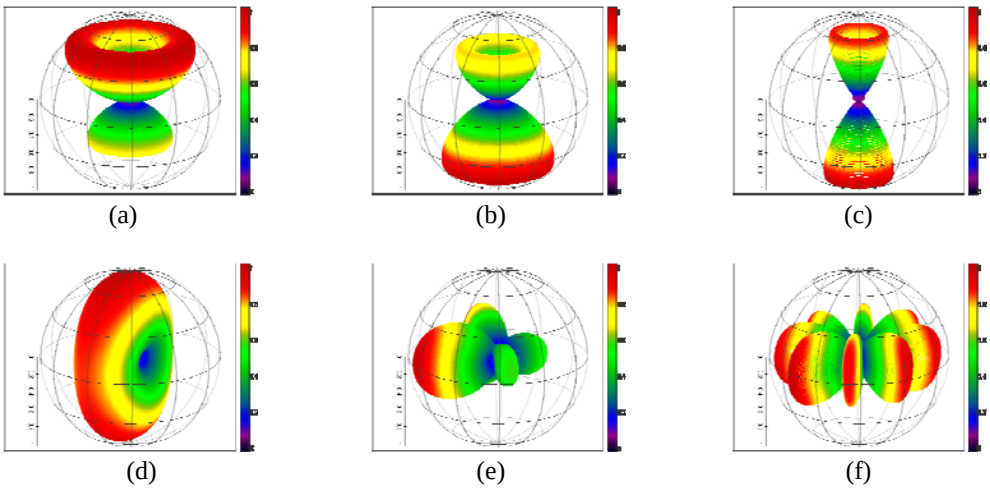

Figure 5. Far-field radiation patterns in the case of the graphene disk excited by the vertical electrical dipole; on-axis dipole location, r_0 = 0; f = 3.1368 THz (a), f = 4.5512 THz (b), f = 9.3182 THz (c) and shifted dipole location, r_0 = 0.9a; f = 1.5425 THz (d), f = 2.3071 THz (e), f = 8.9016 THz (f)

b) Sandwiched disk

For the numerical study of the electromagnetic excitation of a sandwich-like GDG disk we consider the on-axis horizontal magnetic dipole as a source of the incident field (Fig. 6). The dipole is located at the disk axis elevated by the distance $h = 0.055a$. We consider a sandwich-like disk with the radius 50 microns and take the dielectric constant $\varepsilon_r = 60 + i \cdot 0.0006$. The graphene conductivity is taken for the room temperature, with 1-ps electron relaxation time, and several values of the chemical potential.

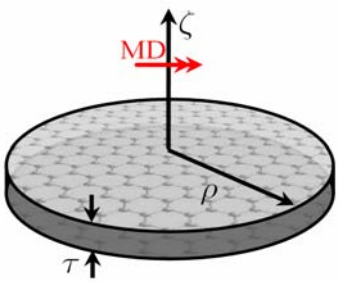

Figure 6. On-axis horizontal magnetic dipole in the presence of the sandwich-like disk

Fig. 7 shows the absolute value of the effective electrical resistivity as a function of normalized frequency *ka* for different

values of chemical potential of the graphene covers. The black curve corresponds to the effective resistivity of a single dielectric disk. One can see that adding graphene covers and increasing its chemical potential leads to the shift of the maximum of the resistivity to the higher frequencies region.

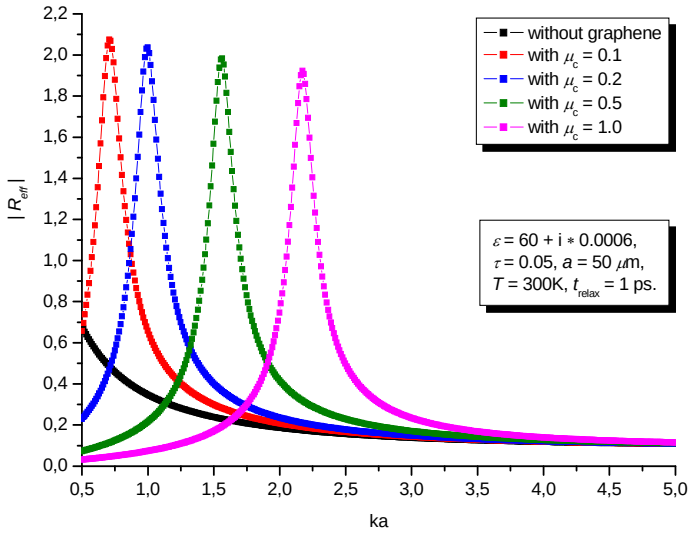

Figure 7. Effective electrical resistivity as a function of normalized frequency

Fig. 8 shows the normalized radiation power of the on-axis horizontal magnetic dipole in the presence of the sandwiched disk as a function of the frequency in terahertz range. One can see the resonance behaviour of the curves. The first low-frequency resonance on each curve (except the black one) corresponds to the surface plasmon mode of the graphene disk. The next resonances correspond to the dielectric disk modes of the "dipole" type, i.e. with several field variations along the radius and one variation along the azimuth. One can see a strong shift of resonance frequencies under variation of the chemical potential.

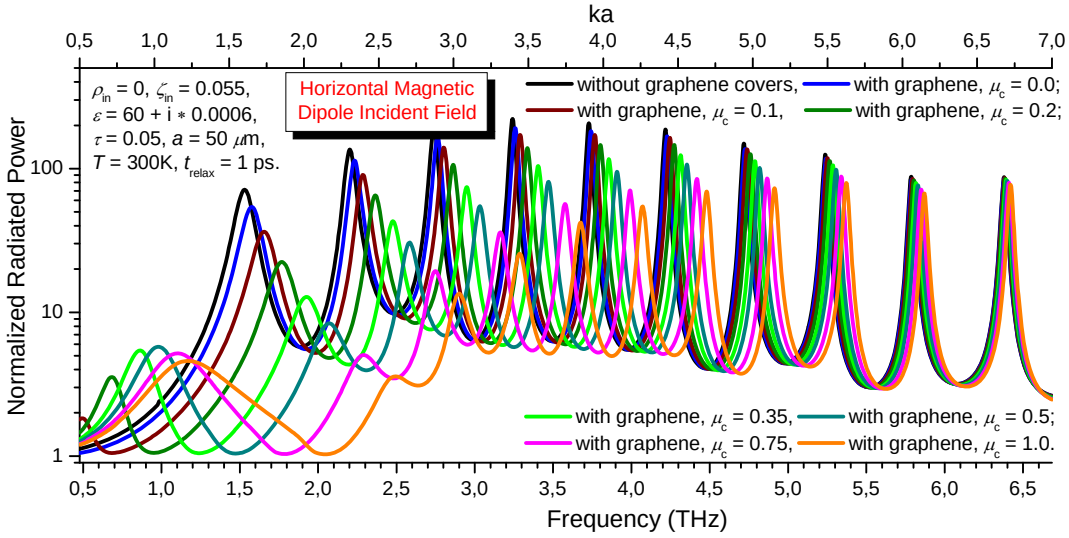

Figure 8. Normalized radiation power of the on-axis horizontal magnetic dipole in the presence of a sandwich-like disk

This research is on-going and we hope that it will lead to a better understanding of all resonance phenomena that are associated to the complicated behaviour of a GDG sandwiched disk as an open resonator in the terahertz range.

As a result of my collaboration with scientists of the University of Nottingham, we have published two conference papers in 2013 (see below). Besides, a few preliminary results have been accepted to publication in a paper submitted to a European journal. Further we plan to prepare a full-length paper corresponding to the project work. It will study plasmon resonances, their near fields and the sandwich-like GDG disk eigenmodes with the aim of possible application of such a resonator in terahertz frequency filters and biosensors. We also plan to expand this work to the graphen-based terahertz antennas.

3) Projected publications / articles resulting or to result from the grant *(ESF must be acknowledged in publications resulting from the grantee's work in relation with the grant)*

1) M.V. Balaban, A. Vukovic, T.M. Benson, A.I. Nosich, "Accurate numerical study of graphene disk surface plasmon resonances," *Proc. Int. Conf. Electronics and Nanotechnology (ELNANO-2013),* Kiev, 2013, pp. 73-75.

2) M.V. Balaban, A. Vukovic, T.M. Benson, "Electromagnetic wave scattering by a graphene-sandwiched dielectric disk analyzed using the generalized boundary conditions," *Proc. Int. Symp. Physics and Engineering of Microwaves, MM, and Sub-MM Waves (MSMW-13),* Kharkiv, 2013, pp. 237-239.

3) M.V. Balaban, O.V. Shapoval, A.I. Nosich, "THz wave scattering by a graphene strip and a disk in free space: integral equation analysis and surface plasmon resonances," *IOP J. of Optics,* vol. 15, no 12, 2013, will be published in Special Issue on Graphene Nanophotonics.

4) Planned: "Excitation of a graphene-sandwiched dielectric disk as a terahertz-range resonator," by M.V. Balaban, et al.

4) Planned: "Integral equation analysis of a graphene-disk terahertz antenna on a substrate backed with graphene plane: radiation efficiency, surface plasmons and tunability," by M.V. Balaban, et al.